THE JOURNAL OF BIOLOGICAL CHEMISTRY
Vol. 274, No. 14, Issue of April 2, pp. 9564–9572, 1999

Printed in U.S.A.

Motile Properties of the Kinesin-related Cin8p Spindle Motor Extracted from *Saccharomyces cerevisiae* Cells*

(Received for publication, November 12, 1998, and in revised form, January 25, 1999)

Larisa Gheber‡§, Scot C. Kuo¶, and M. Andrew Hoyt‡‖

From the ‡Department of Biology, Johns Hopkins University, Baltimore, Maryland 21218 and the ¶Department of Biomedical Engineering, Johns Hopkins School of Medicine, Baltimore, Maryland 21205

We have developed microtubule binding and motility assays for Cin8p, a kinesin-related mitotic spindle motor protein from *Saccharomyces cerevisiae*. The methods examine Cin8p rapidly purified from crude yeast cell extracts. We created a recombinant form of *CIN8* that fused the biotin carrying polypeptide from yeast pyruvate carboxylase to the carboxyl terminus of Cin8p. This form was biotinated in yeast cells and provided Cin8p activity *in vivo*. Avidin-coated glass surfaces were used to specifically bind biotinated Cin8p from crude extracts. Microtubules bound to the Cin8p-coated surfaces and moved at 3.4 ± 0.5 μm/min in the presence of ATP. Force production by Cin8p was directed toward the plus ends of microtubules. A mutation affecting the microtubule-binding site within the motor domain (*cin8-F467A*) decreased Cin8p's ability to bind microtubules to the glass surface by >10-fold, but reduced gliding velocity by only 35%. The *cin8–3* mutant form, affecting the α2 helix of the motor domain, caused a moderate defect in microtubule binding, but motility was severely affected. *cin8-F467A* cells, but not *cin8–3* cells, were greatly impaired in bipolar spindle forming ability. We conclude that microtubule binding by Cin8p is more important than motility for proper spindle formation.

Eukaryotic chromosome segregation is mediated by the mitotic spindle, a microtubule-based motile structure that undergoes a distinct program of morphological changes. It is now clear that many spindle movements are accomplished by microtubule-based motor proteins. Perhaps the best characterized type of spindle motor is that of the BimC subfamily of kinesin-related proteins. Members of the BimC family, first discovered in *Aspergillus nidulans* (1), have been found in numerous eukaryotic species (2–7). These proteins are conserved in amino acid sequence of the motor (force-producing) domain and apparently perform similar roles in many different cell types (8–10). BimC motors are required for bipolar spindle assembly; elimination of their function blocked this essential early mitotic step in fungal, insect, and mammalian cells. The yeast *Saccharomyces cerevisiae* expresses two BimC-related motors that overlap in function, Cin8p and Kip1p. Although neither is individually essential, one of the pair is required for viability (3, 4, 11). Loss of *KIP1* causes less severe phenotypes than loss of *CIN8*, suggesting that Cin8p is more important for successful yeast spindle function (3). Besides essential roles in spindle assembly, Cin8p and Kip1p are also required for the maintenance of spindle bipolarity following assembly and are responsible for producing most of the spindle-elongating force during anaphase (11, 12).

In addition to genetic experiments, several lines of evidence suggest that BimC motors act by cross-linking and sliding antiparallel microtubules found in the spindle midzone. BimC motors have been localized exclusively to the microtubules that lie between the spindle poles (3, 4, 13–15). *In vitro*, BimC motors from *Drosophila melanogaster* and *Xenopus laevis* have been found to move exclusively toward microtubule plus ends, albeit at a rate much slower than that achieved by kinesin (~2 μm/min *versus* 20–40 μm/min for kinesin) (16). In particular, the "bipolar" molecular structure determined for the *Drosophila* BimC motor Klp61F suggested a mechanism by which these motors may contribute to spindle structure and elongation. Klp61F is an elongated bipolar homotetramer, with two motor domains positioned at each end of a rodlike structure (17). Such a bipolar molecule would have the ability to cross-link and slide antiparallel microtubules (10). Despite these suggestive observations, the actual molecular role of BimC motors during spindle dynamics has yet to be established.

In this study, we developed *in vitro* assays for the analysis of the *S. cerevisiae* Cin8p motor. Our purpose was 2-fold. First, the *in vitro* properties of Cin8p have not been described. Mere analogies to other BimC members are clearly indirect and unsatisfactory. Second, the ease of genetic and cell cycle manipulations in yeast demands a similarly direct method to examine and dissect Cin8p functions *in vitro*. Although exogenous expression of motors allows initial reconstituted studies, only endogenous expression in yeast allows direct study of Cin8p cell cycle regulation and different mitotic roles. With these goals in mind, we developed a rapid assay for the activity of Cin8p expressed in yeast cells. For a one-step purification and adsorption to avidin-coated surface, the Cin8 protein was fused to a peptide (biotin carrier peptide or BCP) that is endogenously biotinated in yeast. Subsequent analysis could distinguish microtubule binding from translocation activities, and photoactivation of caged-ATP further increased the sensitivity of our assays. Using these assays, the study of two Cin8p mutants revealed the relative importance of binding and motility for Cin8p *in vivo* functions.

MATERIALS AND METHODS

Yeast Strains and Media—The *S. cerevisiae* strains used in these experiments are derivatives of S288C and are listed in Table I. The *cin8::HIS3* and *kip1::HIS3* alleles were described previously (12). Rich (YPD) and minimal (SD) media were as described by Sherman *et al.* (18). To derepress galactose-inducible genes, cells were grown in 2% raffinose minimal media at 26 °C for 24 h prior to induction by the addition of galactose to 2%. Cycloheximide (Sigma) was added to a final concentration of 5 μg/ml. All media for expression of biotinated Cin8p

* This work was supported by National Institutes of Health Grant GM40714 (to M. A. H.). The costs of publication of this article were defrayed in part by the payment of page charges. This article must therefore be hereby marked "*advertisement*" in accordance with 18 U.S.C. Section 1734 solely to indicate this fact.

§ Supported by Fulbright and Rothschild postdoctoral fellowships.

‖ To whom correspondence should be addressed: Dept. of Biology, Mudd Hall, Johns Hopkins University, 3400 N. Charles St., Baltimore, MD 21218. Tel.: 410-516-7299; Fax: 410-516-5213; E-mail: hoyt@jhu.edu.

TABLE I
Yeast strains and plasmids

Yeast strains and plasmids	Genotype
MAY591	MATα *lys2 his3 leu2 ura3*
MAY2063	*MATa ade2 lys2 his3 leu2 ura3 cin8::URA3*
MAY2180	*MATa ade2 lys2 his3 leu2 ura3 cyh2 can1 kip1::HIS3*
MAY2330	*MATa lys2 his3 leu2 ura3 kip1::HIS3 cin8–3*
MAY3789	*MATa ade2 lys2 his3 leu2 ura3 cin8::HIS3 kip1::HIS3 cyh2* (pMA1208)
MAY4816	*MATa ade2 his3 leu2 ura3* (pFC56)
MAY6013	*MATa ade2 lys2 his3 leu2 ura3 cin8::HIS3 kip1::HIS3 cyh2* (pLG3)
MAY6014	*MATa ade2 lys2 his3 leu2 ura3 cin8::HIS3 kip1::HIS3 cyh2* (pMA1260)
MAY6015	MAY591 (pLG8)
MAY6016	MAY591 (pTK18)
MAY6017	*MATa ade2 lys2 his3 leu2 ura3 cyh2 can1 kip1::HIS3 cin8-F467A*
MAY6018	*MATa ade2 lys2 his3 leu2 ura3 cin8::HIS3 kip1::HIS3 cyh2* (pLG20)
MAY6019	MAY2063 (pLG8)
MAY6020	MAY2063 (pLG15)
MAY6021	MAY2063 (pLG36)
MAY6022	MAY591 (pFC54)
MAY6023	MAY591 (pLG34)
MAY6024	MAY591 (pLG16)
pFC54	P_{GAL} > *KIP3 HIS3 CEN*
pFC56	P_{GAL} > *KIP2 LEU2 CEN*
pLG3	*CIN8-BCP LYS2 CEN*
pLG8	P_{GAL} > *CIN8-BCP LYS2 CEN*
pLG15	P_{GAL} > *cin8-F467A-BCP LYS2 CEN*
pLG16	P_{GAL} > *cin8-R394,H396A-BCP LYS2 CEN*
pLG20	*CIN8-BCP URA3 2μ*
pLG24	P_{GAL} > *cin8–871-BCP LYS2 CEN*
pLG36	P_{GAL} > *cin8–3-BCP LYS2 CEN*
pMA1208	*CIN8 LEU2 CYH2 CEN*
pMA1260	*CIN8 LYS2 CEN*
pTK18	P_{GAL} > *CIN8 LYS2 CEN*

were supplemented with 24 mg/liter biotin (Sigma) (19). Cells were synchronized in G_1 phase by the addition of 4–6 μg/ml of α-factor (Bachem) to liquid media (pH 4), for about 4 h until >85% were unbudded.

DNA Manipulations—To create a biotinated version of Cin8p, we used the polymerase chain reaction to amplify the sequence of yeast *PYC1*, encoding the last 90 amino acids of pyruvate carboxylase (20, 21), and add *Not*I sites at each end. The 5′ side primer used was AATAAAAGCGGCCGCACTGTTACTAAATCCAAAGCA, and the 3′ primer was AATAAATGCGGCCGCTGCCTTAGTTTCAACAGG. The *BCP* fragment was inserted into a *Not*I site that had previously been created at the 3′-end of *CIN8*[1] in the CEN vector pRS317, (22), creating pLG3. Standard DNA manipulations were used to place *CIN8-BCP* under the control of the galactose-inducible promoter on a CEN vector (pLG8). The *cin8–3 (cin8-R196K)* mutation was introduced into *CIN8-BCP* constructs using an *Msc*I to *Pst*I fragment containing the mutant allele. The presence of *cin8–3* was confirmed by sequencing. The *cin8-F467A* mutation was created by the unique site elimination method (23). The primer for mutagenesis was GTCAATTTCGATTCACGGGCAGGTATATGGCCGCTTTTATC, which also introduced a *Bsp*MI site with the amino acid change. The presence of the *cin8-F467A* mutation was confirmed by digestion with *Bsp*MI.

Yeast Extracts and Protein Analysis—Yeast protein extracts for SDS gel electrophoresis were prepared by vortexing cells with glass beads (diameter of 425–600 μm) in 50 mM Tris-HCl (pH 7.4), 250 mM NaCl, 50 mM NaF, 5 mM EDTA, 1 mM phenylmethylsulfonyl fluoride. Cells were vortexed eight times at the maximum speed for 15 s, with 15 s on ice in between. Lysates was separated from cell debris and glass beads via centrifugation for 5 min in the cold. An aliquot was reserved for protein concentration determination using the BCA assay (Pierce) to ensure equal protein loading in gel lanes. Samples were run on 7% acrylamide gels, and the proteins were transferred to polyvinylidene difluoride Immobilon-P (Millipore Corp.) membranes using standard techniques (24). Reagents for immunoblot analysis, including streptavidin-conjugated alkaline phosphatase, were obtained from Tropix. Band intensities were quantified by scanning film images of blots and analyzing with commercial software, IDL (Research Systems).

For the *in vitro* assays, 20–50-ml cultures were grown to midlog phase. Cells were pelleted, washed, and ground with a mortar and pestle under liquid nitrogen in 1 ml of motility buffer 1 (MB1): 30 mM Tris, 35 mM PIPES, final pH 7.2, 175 mM NaCl, 2 mM EDTA, 1 mM EGTA, 10% glycerol, 1 mM phenylmethylsulfonyl fluoride, and 1 mM dithiothreitol. Extracts were clarified by centrifugation at 13,000 rpm in a microcentrifuge at 4 °C. Protein concentration in these extracts was typically 1–3 mg/ml.

In Vitro Microtubule Binding and Motility Assays—To assay Cin8p-BCP-induced microtubule gliding and binding on avidin- or streptavidin-coated surfaces, we modified the protocol of Berliner *et al.* (25). Acid-treated number 1 borosilicate glass coverslips were prepared by overnight incubation in Chromerge (Thomas Scientific), followed by washing under running filtered deionized water for 20–30 min and spin-dried on a custom coverslip spinner. Flow chambers (~10 μl) were formed between microscope slide and the coverslip mounted with double stick tape. For side-by-side comparison of different conditions, up to four chambers separated by silicone grease lines were prepared on a single slide and coverslip. All incubations below were for 10 min at room temperature. Biotinamidocaproyl bovine albumin (Sigma), 10 μl of a 1.7 mg/ml solution in H_2O, was introduced to the chambers, incubated, and washed twice with H_2O. The chambers were treated with 10 μl of 5 mg/ml UltraAvidin™ (deglycosylated and charge-neutralized avidin; from Leinco Technologies) in 10 mM Tris, pH 8, 1 mM EDTA, incubated, and rinsed twice with H_2O, incubated with casein (up to 5 mg/ml) in H_2O, rinsed twice with H_2O, and then rinsed twice with MB1. Crude yeast extracts, 10 μl of 0.2–1 mg/ml total protein, were introduced, incubated for 4–6 min, and washed twice with MB1. In experiments in which the ability of biotin to block binding was assessed, the H_2O rinse after UltraAvidin incubation was replaced with biotin-saturated H_2O, and the consecutive rinses and incubations contained a 1% dilution of biotin-saturated H_2O. The final rinse in MB1 and motility and binding assays were performed without the addition of biotin. For motility, taxol (40 μM)-stabilized microtubules (0.05 mg/ml) in MB1 were added to the flow chamber along with 1–5 mM ATP. Average microtubule length was 5 μm. When tested, other nucleotides were added to a final concentration of 1 mM. For motility assays, MB1 was supplemented with 5 mM $MgSO_4$. To visualize microtubules, video-enhanced DIC microscopy was used as described previously (26). Briefly, an inverted Zeiss microscope (Axiovert 100TV, 100× Plan Neofluar 1.3 NA objective) was modified by installing high transmission polarizers to project images onto a Newvicon camera (Dage VE1000), and images were enhanced using an image processor (Hamamatsu Argus 100). Video sequences were recorded on sVHS tape (Panasonic AG7650 recorder), and microtubule gliding velocities were measured using custom software (Imaging Technologies AFG image processor) from these videos.

ATP uncaging experiments were done in the presence of 1 mM of

[1] T. Kingsbury and M. A. Hoyt, unpublished results.

NPE-ATP[2] (Molecular Probes, Inc., Eugene, OR), a "caged" nucleotide from which ATP is liberated by exposure to UV irradiation. The assay was performed similarly to experiments with myosin (27, 28). Photoactivation of caged ATP required a custom dichroic (400DCLPL from Chroma Technology Corp.) to reflect light from a 75-watt xenon arc lamp. To prevent uncaging during video-enhanced differential interference contrast microscopy, the mercury arc illumination passed through an OG515 Schott Glass optical filter as well as through a 546-nm interference filter. UV illumination of the sample was between 1 and 2 min, followed by observation of the sample for an additional minute. Under these conditions, no effect on the length of microtubules was observed.

Polarity-marked microtubules were prepared according to Refs. 29 and 30 by using a 1:1 ratio of NEM-treated to NEM-untreated tubulin with a total tubulin concentration of 2 μg/ml. Sea urchin (*Strongylocentrotus purpuratus*) axonemes (a gift from Herb Miller and Jennifer Gregory) were used as seeds and were prepared by the method of Bell *et al.* (31) as modified by Walker *et al.* (32). The correct orientation of microtubules labeling was confirmed by a motility assay using bovine brain kinesin (Cytoskeleton).

The microtubule bundling assay was performed using flow chambers constructed as described above. Yeast cell extracts (4 μl of 2 mg/ml) were mixed with taxol-stabilized microtubules in MB1 (16 μl of 3.3 μg/ml). Bundling was observed in solution and on the glass surface by video-enhanced differential interference contrast optics.

RESULTS

A Biotinated Form of Cin8p Provides Activity in Vivo—For this study, we developed an *in vitro* assay to examine the microtubule binding and motile properties of the Cin8p kinesin-related motor from *S. cerevisiae*. We constructed a version of *CIN8* that encodes a fusion between Cin8p and a peptide from *S. cerevisiae* pyruvate carboxylase (product of *PYC1*; Refs. 20 and 21) attached to the Cin8p carboxyl terminus. This region of pyruvate carboxylase, derived from its carboxyl terminus, acts as a covalent acceptor of biotin from a specific ligase (20, 25). We refer to this region of pyruvate carboxylase as BCP for biotin-carrying polypeptide. Fusion proteins that contained the homologous region of *E. coli* pyruvate carboxylase become endogenously biotinated both in *E. coli* and *S. cerevisiae* (19). The *CIN8-BCP* fusion gene was cloned into low copy centromere-containing (CEN) and high copy (2-μm origin) vectors and was expressed from either the endogenous *CIN8* promoter or a high level galactose-inducible promoter. Relative to the level of expression provided by the endogenous promoter/CEN plasmid construct, the endogenous promoter/2-μm version and the galactose promoter/CEN version (induced for 4 h) produced approximately 35- and 500-fold more Cin8p-BCP, respectively.

On account of overlapping functions (3, 4), the ability of *CIN8-BCP* to complement a *CIN8* deletion allele was tested in a strain that was deleted for both *CIN8* and *KIP1*. Since *cin8*Δ *kip1*Δ double mutants are not viable, the viability of the tester strain was maintained by a *CIN8* plasmid that also carried *CYH2*. Despite the presence of a recessive *cyh2* cycloheximide resistance allele in the genome, this strain is sensitive to cycloheximide due to the dominant *CYH2* allele carried on the plasmid (Fig. 1*A*). Transformation with a second plasmid carrying *CIN8-BCP*, however, allowed cells to live without the *CIN8-CYH2* plasmid and therefore to grow on cycloheximide-containing media. This indicated that *CIN8-BCP* provides *CIN8* activity. The *cin8*Δ *kip1*Δ (*CIN8-BCP* plasmid) cells were indistinguishable from *cin8*Δ *kip1*Δ (*CIN8* plasmid) cells for growth rate and temperature resistance. In addition, we found that Cin8p-BCP localized to spindle microtubules in a manner indistinguishable from Cin8p (data not shown). We conclude that Cin8p-BCP acts similarly to Cin8p *in vivo*.

[2] The abbreviations used are: NPE-ATP, P^3-(1-(2-nitrophenyl)ethyl)-ester; AMP-PNP, adenosine 5′-(β,γ-imino)triphosphate

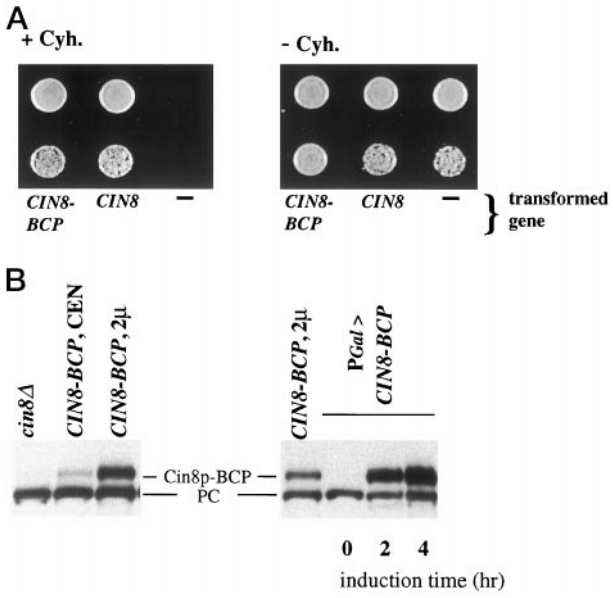

FIG. 1. **Cin8p-BCP is biotinated in yeast cells and complements the function of wild-type Cin8p.** *A*, viability on medium supplemented with or without cycloheximide (*Cyh*). Growth on cycloheximide medium indicates the ability of the *CIN8* form transformed, indicated on the bottom, to rescue the viability of *cin8*Δ *kip1*Δ cells. The *lower spot* in each column is a 100-fold dilution of the *upper spot*. *B*, Western blots of crude yeast extracts run on 7% SDS-acrylamide gel and probed with streptavidin-conjugated alkaline phosphatase. *Left*, extracts are from cells that are either deleted for *CIN8* or expressing Cin8p-BCP from its own promoter carried on a low copy centromere-containing (CEN) or high copy 2 μm-based (2μ) plasmid. The ~128-kDa band, absent from the *cin8*Δ strain, is consistent with the predicted size of Cin8p-BCP. *Right*, comparison between levels of biotinated Cin8p under different expression conditions. Cin8p-BCP expressed either from the P_{GAL} promoter or from its own promoter carried on a high copy (2μ) plasmid. For galactose induction, cells were grown overnight in medium containing raffinose. At $t = 0$, 2% galactose was added to the cultures. Crude extracts were prepared at the indicated time points. Relative to the level of expression provided by the endogenous promoter/CEN plasmid construct, the endogenous promoter/2-μm version and the galactose promoter/CEN version (induced for 4 h) produced approximately 35- and 500-fold more Cin8p-BCP, respectively (determined by scanning of film image of blot). The positions of Cin8p-BCP and pyruvate carboxylase (*PC*) are indicated. Strains utilized were as follows: MAY3789, -6013, and -6014 (*A*); MAY2063, -6013, -6015, and -6018 (*B*).

The Cin8p-BCP fusion protein was endogenously biotinated in *S. cerevisiae* (Fig. 1*B*). Biotination was detected by gel electrophoresis of total cell protein extract followed by blotting and probing with streptavidin-conjugated alkaline phosphatase. In cells expressing *CIN8-BCP* from the galactose-inducible promoter (on a CEN plasmid), the addition of galactose resulted in the appearance of an ~128-kDa protein, consistent with the predicted molecular weight of the fusion protein (Fig. 1*B*). This protein band increased in intensity with the time of galactose induction and was absent from cells that are deleted for *CIN8* (Fig. 1*B*). In cells expressing *CIN8-BCP* from its native promoter, either on low copy (CEN) or high copy (2-μm) plasmids, the amount of Cin8p-BCP produced was correspondingly lower (Fig. 1*B*). The 2-μm expression level was intermediate between that of CEN and P_{GAL} expression levels (Fig. 1*B*). The noninducible biotinated protein band of ~120 kDa is probably *S. cerevisiae* pyruvate carboxylase, one of the five endogenously biotinated proteins in this organism (33).

Bundling of Microtubules in Extracts Containing High Levels of Cin8p—We observed that extracts from yeast cells overproducing Cin8p exhibited a microtubule bundling activity (Fig. 2 and Table II). This activity may be related to the ability of BimC motors to cross-link spindle microtubules (10). When extracts from cells overproducing Cin8p or Cin8p-BCP under

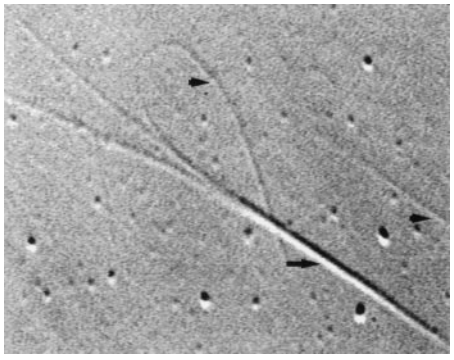

FIG. 2. **Microtubule bundling by Cin8p-BCP.** Crude yeast extract from cells that overexpress Cin8p-BCP were mixed with taxol-stabilized microtubules. Bundled (*arrow*) and single microtubules (*arrowheads*) can be observed. The strain utilized was MAY 6015.

TABLE II
Bundling of microtubules by Cin8p

Protein expressed (expression method)[a]	Nucleotide added	Extent of bundling[b]
		%
Cin8p (P_{GAL})	None	85
Cin8p (P_{GAL})	AMP-PNP	90–95
Cin8p-BCP (P_{GAL})	None	85
Cin8p-BCP (P_{GAL})	AMP-PNP	90–95
Cin8p-BCP (P_{GAL}) + avidin	AMP-PNP	90–95
Cin8p-BCP (2 μm)	None	~0
Cin8p-BCP (2 μm)	AMP-PNP	30
Cin8p (CEN)	AMP-PNP	~0
*cin8*Δ	AMP-PNP	~0
Kip2p (P_{GAL})	AMP-PNP	~0
Kip3p (P_{GAL})	AMP-PNP	~0
Cin8-R394A,H396Ap (P_{GAL})	AMP-PNP	~0
Cin8–871p (P_{GAL})	AMP-PNP	~0

[a] The indicated protein was expressed from its endogenous promoter on a low copy centromere plasmid (CEN), its endogenous promoter on a high copy 2-μm plasmid, or the galactose promoter (P_{GAL}) on a low copy centromere plasmid. The strains utilized are MAY2063, -4816, -6013, -6015, -6016, -6022, -6023, and -6024.

[b] The percentage of observed microtubule structures that were clearly bundled (as opposed to single microtubules).

the control of the galactose promoter were mixed with taxol-stabilized microtubule, bundles were observed. In the presence of 1 mM AMP-PNP, a nonhydrolyzable ATP analogue, 90% of the observable microtubule structures were bundles. Bundles were found in 70–80% of scored microscope fields (n = 100 fields of 400 μm (2). Without the addition of AMP-PNP, the degree of bundling was slightly reduced. At lower overexpression levels (Cin8p-BCP from its normal promoter but on a high copy 2-μm plasmid) bundling was observed, but at a reduced level (Table II). No bundling was observed using extracts from yeast producing wild-type levels of Cin8p or deleted for *CIN8* ($n > 100$ fields for each). We found that the addition of avidin, which interacts with the biotin moiety of BCP, did not alter the extent of Cin8p-BCP-specific bundling. This indicates that the ability of Cin8p-BCP to interact with microtubules is independent of its interaction with avidin. When 1 mM ATP was added to bundles formed in the absence of added nucleotides, dissolution of bundles occurred within 5–10 min. In some cases, we were able to observe the sliding apart of bundles following the addition of ATP. The relative polarity of the sliding microtubules (parallel *versus* antiparallel) was not determined, however.

The bundling in crude cell extracts was specific for overproduced Cin8p. Under the conditions described above, extracts from cells that overproduced either a Cin8p motor domain mutant (Cin8p-R394A, H396A) or kinesin-related Kip2p or Kip3p never bundled microtubules. Interestingly, Cin8p-871, a tail deletion mutant that forms a dimer instead of the wild-type tetramer,[3] was unable to form bundles. This suggests that bundling reflects the ability of BimC motors to cross-link microtubules via their bipolar arrangement of motor domains.

Cin8p-BCP Specifically Binds Microtubules to Avidin-coated Surfaces—Avidin-coated glass coverslips were used to specifically bind Cin8p-BCP from crude protein extracts. Two criteria were used to establish that any observed microtubule binding to these surfaces was specific for Cin8p: 1) extracts that lack biotinated Cin8p should exhibit no microtubule binding, and 2) added biotin should block microtubule binding. Fig. 3 summarizes six experiments in which microtubule binding was assessed in the absence of added nucleotide. The microtubule binding activity was high from extracts in which Cin8p-BCP was overproduced but was greatly reduced by the addition of biotin or from extracts of *cin8*Δ cells or cells overexpressing Cin8p (without the BCP tag). The main factors that influenced the specificity of this assay were ionic strength and the concentration of casein, which was used to block nonspecific interactions. We found that different extracts from the same yeast strain sometimes required different casein concentrations to block nonspecific microtubule binding. Therefore, for every extract preparation we determined the casein concentration that, in the absence of added nucleotide, would allow high microtubule binding in the absence of a biotin block and very low binding in the presence of a biotin block. Reducing NaCl concentrations below 150 mM also increased the nonspecific binding of microtubules. However, NaCl concentration above 200 mM interfered with binding of microtubules to Cin8p. The optimal conditions were achieved with 175 mM NaCl in the buffers for both extract preparation and assays. The number of specifically bound microtubules was higher on modified avidin (UltraAvidin™; see "Materials and Methods") surfaces than on other avidin- and streptavidin-coated surfaces.

In Vitro Motile Activity of Cin8p—The spindle pole-separating activity of Cin8p is most easily explained by a plus end-directed motile activity (3, 12, 34). To observe Cin8p motility *in vitro*, 1 mM ATP was added to microtubules preadsorbed to Cin8p-BCP on avidin-coated surfaces. The Cin8p-BCP source for these initial experiments was an extract from cells in which it had been overproduced from the galactose promoter. Under these conditions, efficient microtubule gliding was observed (Fig. 4*A*). Of the 3–10 microtubules visible per 400-μm (2) field, 70–80% moved in the presence of ATP. The nonmotile microtubules divided approximately equally between two categories: immobile microtubules and those that detached. For about 10–20% of the moving microtubules, pivoting around a single point on the surface was observed during movement. Such movement probably reflects the activity of a single surface motor (35). For about 10% of the moving microtubules, the movement was episodic, where changes in velocity or stops and starts were observed. Buckling of microtubules, which would indicate the presence of binding but nonmotile motors on the surface (36), was not observed.

To determine the directionality of Cin8p-induced motility, we used minus end-marked microtubules nucleated from sea urchin sperm axonemes (see "Materials and Methods"). The direction of all gliding microtubules was minus end leading (n = 16), indicating that Cin8p exhibits plus end-directed activity (Fig. 4*B*).

The velocity distribution of Cin8p-induced microtubule gliding is shown in Fig. 5*A*. This distribution represents 85 moving microtubules in tests of four different Cin8p-BCP overproduc-

[3] E. Hildebrandt, L. Gheber, and M. A. Hoyt, unpublished observation.

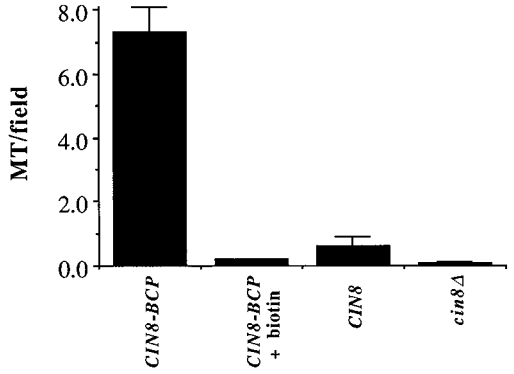

FIG. 3. **Microtubule binding to Cin8p-BCP on glass surfaces.** Extracts were prepared from cells that overexpressed (by P_{GAL}) either biotinated or untagged Cin8p or were deleted for *CIN8*. The *bars* represent the mean ± S.E. of microtubules bound per 400-μm^2 field. For each category, 120 fields were counted (six experiments, 20 fields/category/experiment). For each experiment, one coverslip was divided into four chambers, which each received one of the four indicated extracts (*bottom* of *graph*). Microtubule attachment to the glass surface was measured in the absence of added nucleotides. During adsorption, the total extract protein concentration in each chamber was 1 mg/ml. For blocking with biotin, the chamber surface was saturated with biotin after the adsorption of avidin but prior to the addition of cell extract (see "Materials and Methods"). Strains utilized were MAY2063, -6015, and -6016.

ing extracts. The average velocity of Cin8p-BCP induced gliding was 3.4 ± 0.5 μm/min (S.E. shown in parentheses). A small but significant number of microtubules moved at rates as much as 3 times this average, causing the velocity distribution to be quite broad. The distribution of the overall distance moved by microtubules (running length) is shown in Fig. 5*B*. About 75% of microtubules moved relatively short distances, smaller than 5 μm, before the microtubule either paused or detached from the glass surface. High microtubule densities did not change the episodic nature of movement. The short running length may suggest that Cin8p is less processive than kinesin (37, 38), which was also suggested in a kinetic study on the vertebrate BimC motor Eg5 (39).

The effects of added nucleotide on microtubule binding and gliding are shown in Table III. The number of microtubules found on the surface in the presence of AMP-PNP was more than 10-fold larger than that with ATP. However, unlike experiments that lacked added nucleotide (Table III and Fig. 3), a high fraction of the AMP-PNP-bound microtubules could not be blocked by preincubation with biotin. Nonetheless, this residual microtubule binding with AMP-PNP appeared specific to Cin8p; extracts from *cin8*Δ cells did not show microtubule surface binding in the presence of AMP-PNP. As expected, AMP-PNP did not support any microtubule gliding. With ADP there were fewer bound microtubule than with ATP or AMP-PNP or in the absence of added nucleotide (Table III). This observation is consistent with what is known for conventional kinesin for which affinity to microtubules is strong in the presence of AMP-PNP or in the absence of added nucleotide and is reduced in the ADP-bound state. We also found that 1 mM GTP was unable to support Cin8p-induced motility. GTP supports motility by kinesin at a reduced level relative to ATP (40, 41), but tests on BimC motors have not previously been reported.

The above microtubule binding and motility experiments were performed using extracts in which Cin8p-BCP had been overexpressed. We also used this assay to examine Cin8p activity at closer to normal expression levels. While we have not been able to detect microtubule binding to the glass surface using Cin8p-BCP from cells producing it from its native promoter on a low copy (CEN) plasmid, we have been able to assay Cin8p-BCP activity when produced from its native promoter on a high copy (2-μm) plasmid. Under these conditions, Cin8p levels are ~35-fold higher than wild type but lower than the ~500-fold amplification produced by P_{GAL}. P_{GAL} overexpressed *CIN8* is toxic to cells, but the 2-μm plasmid is tolerated and complements the growth defect of *cin8*Δ *kip1*Δ cells. In addition, Cin8p expression from the 2-μm plasmid resembles the cell cycle-specific fluctuations of Cin8p levels found in the wild-type situation.[4]

Although Cin8p-BCP from 2-μm extracts could immobilize microtubules in the presence of AMP-PNP, introducing ATP released all the bound microtubules before motility could be analyzed (Table III). To overcome this problem, we used NPE-ATP, a "caged" nucleotide from which ATP is liberated by exposure to UV irradiation. Prior to uncaging with UV, microtubules were bound to the surface, similar to the absence-of-nucleotide rigor state. Upon activation with UV light, the pulse of released ATP caused gliding of the preadsorbed microtubules. The motility characteristics in caged ATP protocol were slightly different from the simple ATP addition protocol, described above. In direct comparison with the P_{GAL} extracts, fewer microtubules moved, and running lengths were shorter in the caged ATP experiment. The average running length was 3.3 ± 0.3 and 1.1 ± 0.1 μm for steady ATP and caged ATP, respectively. However, microtubule gliding velocities were similar for P_{GAL} caged ATP, P_{GAL} steady ATP, and 2-μm caged ATP assays (Table III), validating the use of caged ATP to examine Cin8p activity in situations where increased sensitivity is required.

Analysis of Cin8p Motor Domain Mutants in Vivo and in Vitro—An advantage of our experimental system is that it allows us to analyze both the phenotypic and biochemical consequences of motor gene mutations. To demonstrate this potential, we examined two Cin8p forms mutant within their motor domains. One mutant is encoded by *cin8–3*, a form that has been subjected to significant *in vivo* analyses (3, 11, 12). *cin8–3* causes a change from arginine to lysine at amino acid 196, located in the region corresponding to the α2 helix of human kinesin (42). The second mutant form is encoded by *cin8-F467A*, the change occurring within a region corresponding to the kinesin L12 loop, important for microtubule interaction (43). Both mutations cause temperature-sensitive growth at 33° in the absence of the functionally overlapping *KIP1* (data not shown), but both are clearly compromised at room temperature as well (see below). We could detect no difference in the expression level of these two mutant forms compared with wild-type Cin8p when produced at low copy from the *CIN8* promoter (data not shown). Therefore, the phenotypic effects of these mutations can be attributed to the differences in their activities. In the experiments described below, we examined wild-type and mutant forms expressed from P_{GAL} in cells that were deleted for *CIN8*. All analyses were performed at room temperature (~25 °C).

Fig. 6 compares the ability of the Cin8p mutants to bind microtubule *in vitro*. Extracts producing the Cin8p-BCP forms were passed over avidin-coated glass surfaces to adsorb the motor. Microtubules were added in the presence of AMP-PNP, and the number bound per 400-μm (2) field was determined by microscopy. We also determined, by immunoblotting, that all three forms were expressed at comparable levels (Fig. 6*B*) and were bound to the glass surface equally well (data not shown). Cin8p-F467A displayed severely reduced microtubule binding. Even higher expression levels from longer induction times (Fig.

[4] L. Gheber, E. Hildebrandt, and M. A. Hoyt, unpublished observations.

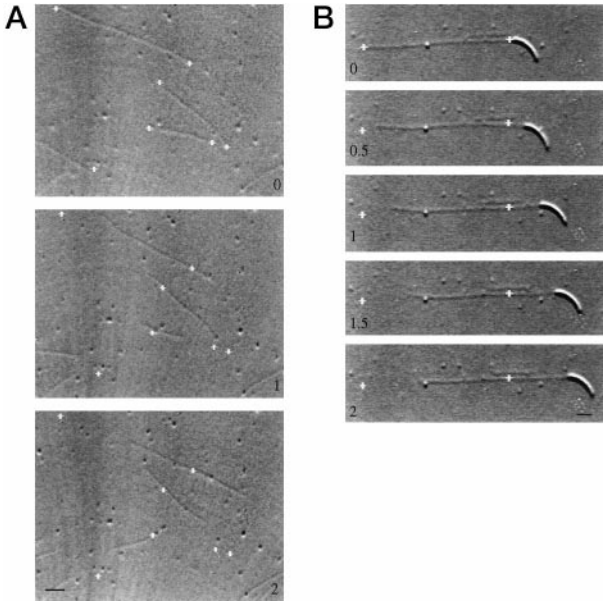

FIG. 4. **Cin8p-BCP-catalyzed microtubule motility.** *A*, time lapse sequence of a field of gliding microtubules driven by Cin8p-BCP bound to a glass surface. The *white crosses* indicate the positions of microtubule ends at the beginning of the sequence. *B*, demonstration that Cin8p exerts force toward the plus ends of microtubules. The microtubule is marked at its minus end by the large structure, a sea urchin axoneme fragment that was used as a seed to grow the microtubule. The leading minus end indicates that Cin8p exerts force toward the plus end. For both *A* and *B*, the *numbers* indicate the elapsed time in minutes, and the bar represents 1 μm. The strain utilized was MAY6015.

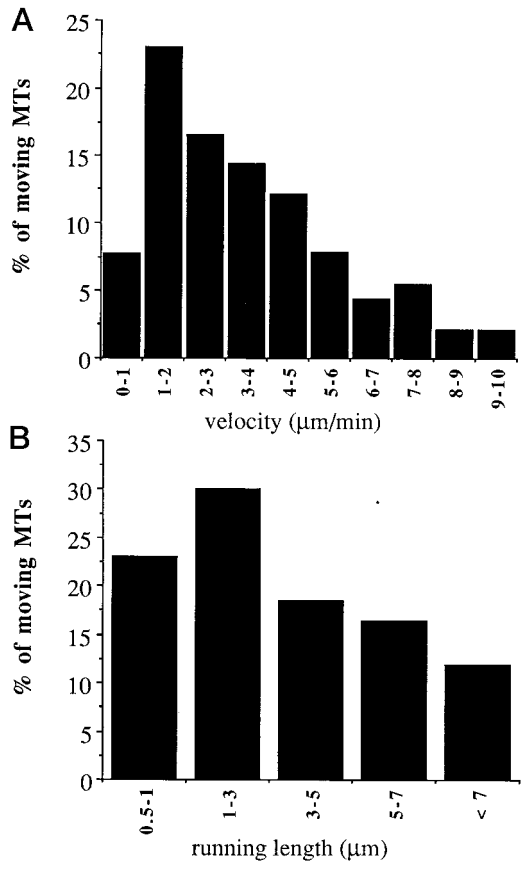

FIG. 5. **Properties of Cin8p-catalyzed microtubule motility.** *A*, velocity distribution of moving microtubules driven by Cin8p-BCP on glass surfaces. *B*, running length of the microtubules measured in *A*. For these data, a total of 85 moving microtubules were measured in four experiments. The strain utilized was MAY6015.

6; 4.5 h of induction) did not rescue the reduction in microtubule binding. Cin8p-3 also exhibited a reduction in microtubule binding, but this was less pronounced (typically ~50% reduced). By optically focusing on the glass surface, we could estimate the rates of microtubule capture and release. For wild-type Cin8p surfaces, almost all microtubules that landed adhered for at least 5 min (the length of the observation time). For Cin8p-F467A and Cin8p-3 surfaces, 30–70% of the landing microtubules rapidly detached (within 1 s). However, of the microtubules that were captured to the mutant surfaces, most remained attached for at least 5 min. This suggests that the reduced microtubule binding affinity of the mutant proteins reflects a diminished capture rate rather than an increased detachment rate.

Because of their reduced ability to capture microtubules, experiments for *in vitro* motility of mutants required the more sensitive caged ATP method (see above). In this set of experiments (Table IV), the average gliding velocity of wild-type Cin8p-BCP measured after uncaging ATP was 2.8 ± 0.5 μm/min, within the margin of error of that measured using ATP (3.4 ± 0.5 μm/min). Although Cin8p-F467A was greatly reduced in its ability to bind microtubules, the gliding velocity achieved was reduced by only 35% (Table IV). In addition, the fraction of surface-bound microtubules that responded to ATP uncaging by either moving or detaching was similar to that of the wild type. This finding, combined with the results in Fig. 6, leads us to conclude that the effect of this mutation is mainly on the ability of Cin8p to bind microtubules rather than on motility. In contrast, for Cin8p-3, ATP uncaging resulted in a lower fraction of microtubules moving or detaching from the surface. However, the few motile microtubules moved at a velocity close to the wild type.

To summarize mutant reconstitution studies, the main defect of Cin8p-F467A mutant was its ability to bind microtubules *in vitro*. In comparison, Cin8p-3 mutant was less impaired for microtubule binding but was able to move fewer microtubules after ATP uncaging.

A major mitotic role for BimC motors is the assembly of the bipolar spindle. By monitoring the extent of spindle bipolarity and pole-to-pole distances, we were able to detect differential effects of the two Cin8p motor mutants on the spindle assembly process (Fig. 7). After release from α-factor block at G_1, synchronized wild-type cells convert monopolar astral arrays of microtubules into short bipolar spindles, which subsequently elongate when cells enter anaphase. In these *in vivo* experiments, we used cells deleted for *KIP1* encoding the functionally overlapping BimC motor. The *CIN8* allelic forms were integrated into the genome and expressed from the native promoter (see "Materials and Methods"). Relative to *CIN8*, the *cin8-F467A* cells were impaired in their ability to form bipolar spindles; monopolar structures took longer to disappear, and bipolar structures took longer to appear (Fig. 7, *A* and *B*). The bipolar spindles formed by *cin8-F467A* also were shorter than *CIN8* (0.5 ± 0.1 *versus* 1.1 ± 0.1 μm). *cin8-F467A* cells were also delayed in their entry into anaphase as evidenced by the delayed appearance of cells with elongated spindles (>2 μm; Fig. 7*C*). In contrast, we could not detect any effect of *cin8–3* on spindle assembly at 25 °C, although this mutant may exhibit a slight anaphase entry delay (Fig. 7, *B* and *C*). Therefore, *cin8-F467A*, but not *cin8–3*, significantly reduces the ability of Cin8p to form bipolar spindles. Further attempts to observe effects on anaphase proficiency were inconclusive, possibly due to the difficulty in separating the contribution of the dynein motor, which also contributes to anaphase pole separation.

TABLE III
Nucleotide specificity of microtubule binding and motility

Expressed form of Cin8p	Nucleotide added	Bound microtubules/field[a]		Motility rate (mean ± SE), *n*
		Without biotin	With biotin	
				μm/min
Cin8p-BCP overexpressed from the P_{GAL} promotor (MAY6015)	No nucleotide	15 ± 2	1.7 ± 0.1	None[b]
	AMP-PNP	60 ± 5	25 ± 6	None
	Caged ATP	9.1 ± 2.1[c]	1.0 ± 0.3[c]	3.2 ± 0.6, 15[d]
	ATP	5.2 ± 0.8	0.5 ± 0.1	3.4 ± 0.5, 85
	ADP	2.0 ± 0.3	0	None
	GTP	6.8 ± 0.3	0.7 ± 0.1	None
Cin8p-BCP, 2 μm (MAY 6018)	AMP-PNP	30 ± 3	12 ± 1	None
	Caged ATP	4.5 ± 0.5[c]	0.5 ± 0.4[c]	3.1 ± 0.5, 14[d]
	ATP	0	ND[e]	ND
*cin8*Δ (MAY2063)	AMP-PNP	0	ND	ND
	Caged ATP	0[c]	ND	ND

[a] Bound microtubules remain stationary on the glass surface. Unbound microtubules diffuse away from the glass surface in less than 1 s.
[b] None, no motility was observed.
[c] In the presence of caged ATP, the number of bound microtubules was determined before uncaging.
[d] Determined after uncaging of ATP.
[e] ND, not determined.

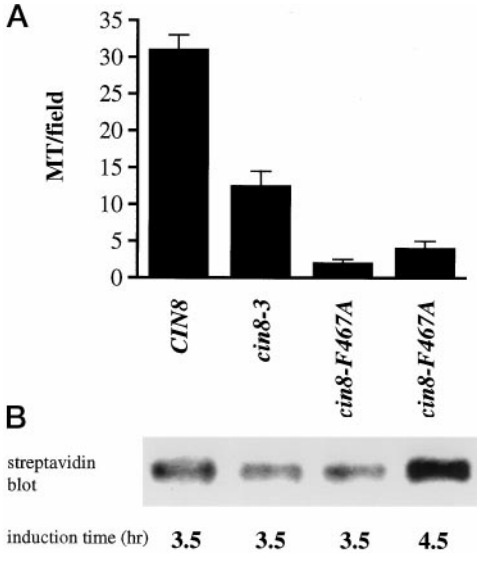

FIG. 6. **Microtubule capture onto glass surfaces by Cin8p and mutant forms.** *A*, binding of microtubules to glass surface in the presence of AMP-PNP. The extracts were made from cells expressing the indicated *CIN8* alleles. The *bars* represent the mean ± S.E. of microtubules bound in 40 (400-μm^2) fields. The values here were corrected by the subtraction of microtubules bound after treatment of the surfaces with biotin (see Table III, AMP-PNP rows for examples). *B*, Western blots of extracts used in *A*, probed with streptavidin-conjugated alkaline phosphatase. The induction time indicates the hours elapsed following the addition of galactose. The strains utilized were MAY6019, -6020, and -6021.

DISCUSSION

The phenotypic analyses of *S. cerevisiae* cells mutant for BimC-related Cin8p have revealed many aspects of the *in vivo* function of this family of mitotic spindle motors (8–10). The observed requirement for Cin8p during spindle assembly and elongation and its localization to microtubules between the spindle poles have led to the suggestion that Cin8p acts to cross-link and slide spindle midzone microtubules. The *in vitro* analysis presented here demonstrates that Cin8p indeed exhibits the properties expected for a kinesin-related microtubule-based motor protein. Cin8p can bind and bundle microtubules in the absence of nucleotide or in the presence of AMP-PNP. In the presence of ATP, Cin8p induced microtubule gliding in a plus end-directed fashion. If Cin8p acts to cross-link antiparallel midzone microtubules, plus end-directed sliding would lead to spindle elongation.

TABLE IV
Microtubule gliding induced by wild-type and mutant Cin8p after ATP uncaging

CIN8 genotype[a]	Motility rate[b] (mean ± S.E.)	Total microtubules[c]	Moving microtubules[b]	Detached microtubules[b]
	μm/min		%	%
CIN8	2.8 ± 0.5 (13)[d]	65	20	20
cin8-F467A	1.8 ± 0.3 (15)	41	37	2
cin8–3	2.3 ± 0.6 (4)	133	3	8

[a] The strains utilized are MAY6019, -6020, and -6021.
[b] Determined after uncaging of ATP.
[c] Determined before uncaging of ATP.
[d] The numbers of moving microtubules measured are shown in parentheses.

The assay we developed examines Cin8p isolated from crude extracts of *S. cerevisiae* cells. An active biotinated form was expressed in *S. cerevisiae* and rapidly isolated by adsorption to an avidin-coated glass surface. In principle, this assay has several advantages over studies of motors produced in exogenous host cells or assays in which extensive purification steps are required. Since Cin8p acts in a cell cycle-specific fashion, it seems likely that its activity will be subject to cell cycle regulation. We have determined that Cin8p levels fluctuate during the cell cycle, peaking in mitosis and rapidly decreasing during the G_1 stage.[5] It is possible that other forms of post-translational regulation are also imposed upon Cin8p. The rapid purification used in this assay, requiring minimal manipulation of the protein extracts, may permit (hypothetical) regulatory proteins to maintain their association with Cin8p, allowing their influence to be monitored. On account of the low intracellular abundance of Cin8p, we were unable to detect Cin8p activity in extracts of cells in which it was produced at normal levels. We were successful, however, with assays using cells harboring the gene (expressed from its normal promoter) in extra copies on a 2 μm-based plasmid. Our crude extract assay is currently being used to examine differences in microtubule binding and translocation proficiency of Cin8p during cell cycle progression.

With our biotin-based assay, we characterized the microtubule binding and motility properties of Cin8p. The nucleotide

[5] E. Hildebrandt, T. Kingsbury, and M. A. Hoyt, unpublished observations.

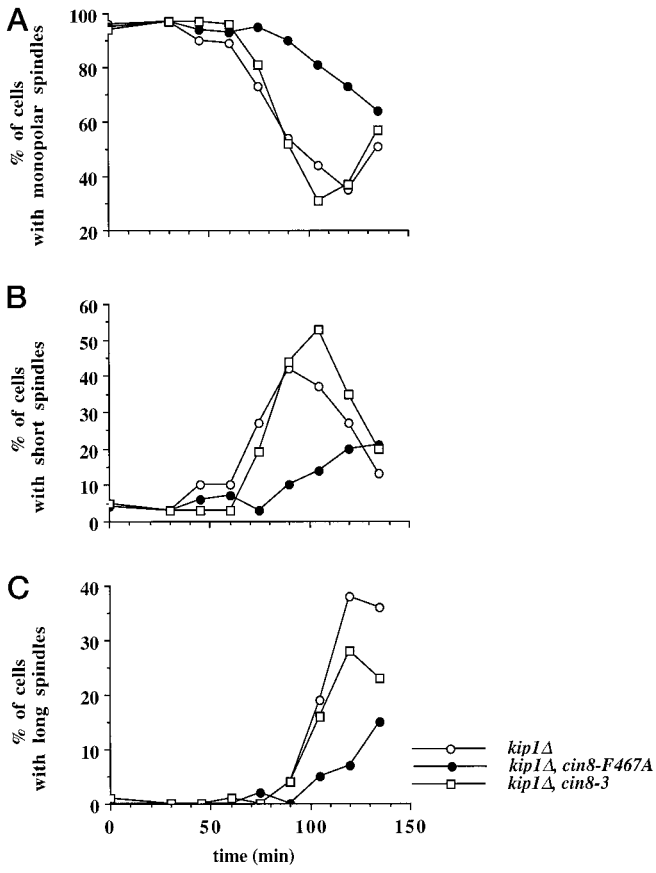

FIG. 7. ***In vivo* spindle assembly proficiency by wild-type and mutant Cin8p forms.** Cells were synchronized in G1 with α-factor and released into fresh media (at room temperature), and aliquots were fixed at the indicated times and observed for microtubule structures by immunofluorescence microscopy. *A*, percentage of total cells with monopolar spindles. *B*, percentage of total cells with short ($\leq$ 2 μm) spindles. *C*, percentage of total cells with long (>2-μm) spindles. ○, *kip1*Δ, strain MAY2180; ●, *kip1*Δ *cin8-F467A*, strain MAY6017; □, *kip1*Δ *cin8–3*, strain MAY2330.

specificity for microtubule binding was similar to that reported for other kinesins and exhibits strong binding in the presence of AMP-PNP and weak binding in the presence of ADP (Table III). Conventional kinesin can move microtubules in the presence of GTP (40, 41), but other kinesin-related proteins, such as Ncd, cannot utilize GTP (44, 45). In our experimental conditions, GTP was unable to support motility by Cin8p.

In our assay, Cin8p produced microtubule gliding rates of ~3.4 μm/min. This rate is approximately 10-fold slower than that produced by kinesin *in vitro* (16) but similar to the 1.0–2.4 μm/min reported for two other BimC motors (15, 46, 47). The distribution of microtubule velocities determined for Cin8p was broad (Fig. 6*A*), ranging between 1 and 10 μm/min (although most fell in the 1–4-μm/min range). A much narrower velocity distribution was reported for the *Xenopus* BimC homologue, Eg5, but this study utilized a fragment of the motor produced in bacteria (47). The specificity of movement in our assay to biotinated Cin8p makes it highly unlikely that other motors were contributing to this broad range of velocities. It is possible, therefore, that Cin8p motors with different motile properties exist in the extracts examined. It is tempting to speculate that the broad velocity distribution reflects cell cycle regulation of the motile properties of Cin8p.

Comparison of Cin8p Mutants in Vivo and in Vitro—Coupled with the *in vivo* assays of spindle motors in *S. cerevisiae*, the rapid *in vitro* assay described here allows a powerful analysis of the properties of mutant motor forms. In this study, we examined the properties of two Cin8p mutants altered within their motor domains. The Cin8p-3 form is altered at an arginine (changed to lysine) that is conserved among kinesin family members. The corresponding residue in human kinesin lies in the motor domain α2, the P-loop helix (42). The role of this helix is not known. In the conditions of our assay, Cin8p-3 was moderately reduced in its ability to bind microtubules and greatly reduced in its ability to move microtubules following ATP uncaging. The ability of Cin8p-3 to form bipolar spindles *in vivo* (at room temperature) was not affected, suggesting that its motility defect does not impair its ability to assemble spindles.

The second mutant, Cin8p-F467A was specifically created in loop L12, which contains residues highly conserved among kinesin-related proteins (42). Mutant analysis of human kinesin revealed that L12 is the major domain for the kinesin-microtubule interaction (43). Changes of two hydrophobic residues in the same region of human kinesin to alanine reduced the microtubule-binding affinity (43). In our assay, the F467A change reduced the number of microtubules bound to the Cin8p surface 10-fold (Fig. 6). Despite the pronounced effect on microtubule binding, the gliding velocity produced by Cin8p-F467A was reduced by only 35% (Table IV). A similar effect was also found for the human kinesin L12 mutants for which the effect on velocity was very mild as compared with the effect on the affinity to microtubule (43). Our findings indicate that the L12 region of Cin8p, like kinesin, is important for microtubule binding. *In vivo*, *cin8-F467A* was found to be defective for bipolar spindle assembly compared with either wild-type or *cin8–3* (at room temperature). Therefore, changes in different motor domain regions can cause different phenotypic effects. In mitosis, Cin8p acts prior to anaphase to assemble spindles and maintain their structural integrity. During anaphase, Cin8p is almost certainly the most important pole-separating motor in *S. cerevisiae* (12). Combined with the mutant study here, we suggest that microtubule binding ability is important for spindle assembly, while force production may be important for anaphase spindle elongation.

In summary, we have developed methods that allow the comparative studies of motor proteins *in vivo* and *in vitro*. In developing these techniques, we anticipate their applicability to the study of other motor proteins. As was the case for Cin8p, tagging with BCP need not interfere with the normal activity of the motor *in vivo*. This allows the examination of functional motor forms rapidly extracted from their endogenous host cell.

Acknowledgments—We thank Tami Kingsbury for providing plasmids and for sequencing the *cin8–3* allele, and we thank Cindy Dougherty and Emily Hildebrandt for critical reading of the manuscript.

REFERENCES

1. Enos, A. P., and Morris, N. R. (1990) *Cell* **60,** 1019–1027
2. Hagan, I., and Yanagida, M. (1990) *Nature* **347,** 563–566
3. Hoyt, M. A., He, L., Loo, K. K., and Saunders, W. S. (1992) *J. Cell Biol.* **118,** 109–120
4. Roof, D. M., Meluh, P. B., and Rose, M. D. (1992) *J. Cell Biol.* **118,** 95–108
5. Heck, M. M., Pereira, A., Pesavento, P., Yannoni, Y., Spradling, A. C., and Goldstein, L. S. (1993) *J. Cell Biol.* **123,** 665–679
6. Le Guellec, R., Paris, J., Couturier, A., Roghi, C., and Philippe, M. (1991) *Mol. Cell. Biol.* **11,** 3395–3398
7. Blangy, A., Lane, H. A., d'Herin, P., Harper, M., Kress, M., and Nigg, E. A. (1995) *Cell* **83,** 1159–1169
8. Hoyt, M. A., and Geiser, J. R. (1996) *Annu. Rev. Genet* **30,** 7–33
9. Barton, N. R., and Goldstein, L. S. (1996) *Proc. Natl. Acad. Sci. U. S. A.* **93,** 1735–1742
10. Kashina, A. S., Rogers, G. C., and Scholey, J. M. (1997) *Biochim. Biophys. Acta* **1357,** 257–271
11. Saunders, W. S., and Hoyt, M. A. (1992) *Cell* **70,** 451–458
12. Saunders, W. S., Koshland, D., Eshel, D., Gibbons, I. R., and Hoyt, M. A. (1995) *J. Cell Biol.* **128,** 617–624
13. Hagan, I., and Yanagida, M. (1992) *Nature* **356,** 74–76
14. Sawin, K. E., and Mitchison, T. J. (1995) *Proc. Natl. Acad. Sci. U. S. A.* **92,** 4289–4293

15. Barton, N. R., Pereira, A. J., and Goldstein, L. S. (1995) *Mol. Biol. Cell* **6,** 1563–1574
16. Bloom, G. S., and Endow, S. A. (1995) *Protein Profile* **2,** 1105–1171
17. Kashina, A. S., Baskin, R. J., Cole, D. G., Wedaman, K. P., Saxton, W. M., and Scholey, J. M. (1996) *Nature* **379,** 270–272
18. Sherman, F., Fink, G. R., and Hicks, J. B. (1983) *Methods in Yeast Genetics*, pp. 61–62, Cold Spring Harbor Laboratory, Cold Spring Harbor, NY
19. Cronan, J. E., Jr. (1990) *J. Biol. Chem.* **265,** 10327–10333
20. Lim, F., Morris, C. P., Occhiodoro, F., and Wallace, J. C. (1988) *J. Biol. Chem.* **263,** 11493–11497
21. Walker, M. E., Val, D. L., Rohde, M., Devenish, R. J., and Wallace, J. C. (1991) *Biochem. Biophys. Res. Commun.* **176,** 1210–1217
22. Sikorski, R. S., and Boeke, J. D. (1991) *Methods Enzymol.* **194,** 302–318
23. Nicolas, G., Pedroni, S., Fournier, C., Gautero, H., and Lecomte, M. C. (1997) *BioTechniques* **22,** 430–434
24. Sambrook, J., Fritsch, E. F., and Maniatis, T. (1989) *Molecular Cloning: A Laboratory Manual*, 2nd Ed., Cold Spring Harbor Laboratory, Cold Spring Harbor, NY
25. Berliner, E., Mahtani, H. K., Karki, S., Chu, L. F., Cronan, J. E., Jr., and Gelles, J. (1994) *J. Biol. Chem.* **269,** 8610–8615
26. Kuo, S. C., Gelles, J., Steuer, E., and Sheetz, M. P. (1991) *J. Cell Sci. Suppl.* **14,** 135–138
27. Goldman, Y. E., Hibberd, M. G., and Trentham, D. R. (1984) *J. Physiol.* (*Lond.*) **354,** 577–604
28. Hibberd, M. G., Goldman, Y. E., and Trentham, D. R. (1984) *Curr. Top. Cell Regul.* **24,** 357–364
29. Koshland, D. E., Mitchison, T. J., and Kirschner, M. W. (1988) *Nature* **331,** 499–504
30. Hyman, A., Drechsel, D., Kellogg, D., Salser, S., Sawin, K., Steffen, P., Wordeman, L., and Mitchison, T. (1991) *Methods Enzymol.* **196,** 478–485
31. Bell, C. W., Fraser, C., Sale, W. S., Tang, W. J., and Gibbons, I. R. (1982) *Methods Cell Biol.* **24,** 373–397
32. Walker, R. A., O'Brien, E. T., Pryer, N. K., Soboeiro, M. F., Voter, W. A., Erickson, H. P., and Salmon, E. D. (1988) *J. Cell Biol.* **107,** 1437–1448
33. Lim, F., Rohde, M., Morris, C. P., and Wallace, J. C. (1987) *Arch. Biochem. Biophys.* **258,** 259–264
34. Saunders, W., Lengyel, V., and Hoyt, M. A. (1997) *Mol. Biol. Cell* **8,** 1025–1033
35. Howard, J., Hudspeth, A. J., and Vale, R. D. (1989) *Nature* **342,** 154–158
36. Hancock, W. O., and Howard, J. (1998) *J. Cell Biol.* **140,** 1395–1405
37. Romberg, L., Pierce, D. W., and Vale, R. D. (1998) *J. Cell Biol.* **140,** 1407–1416
38. Hackney, D. D. (1995) *Nature* **377,** 448–450
39. Crevel, I. M., Lockhart, A., and Cross, R. A. (1997) *J. Mol. Biol.* **273,** 160–170
40. Vale, R. D., Reese, T. S., and Sheetz, M. P. (1985) *Cell* **42,** 39–50
41. Cohn, S. A., Ingold, A. L., and Scholey, J. M. (1989) *J. Biol. Chem.* **264,** 4290–4297
42. Kull, F. J., Sablin, E. P., Lau, R., Fletterick, R. J., and Vale, R. D. (1996) *Nature* **380,** 550–555
43. Woehlke, G., Ruby, A. K., Hart, C. L., Ly, B., Hom, B. N., and Vale, R. D. (1997) *Cell* **90,** 207–216
44. Walker, R. A., Salmon, E. D., and Endow, S. A. (1990) *Nature* **347,** 780–782
45. Shimizu, T., Toyoshima, Y. Y., Edamatsu, M., and Vale, R. D. (1995) *Biochemistry* **34,** 1575–1582
46. Cole, D. G., Saxton, W. M., Sheehan, K. B., and Scholey, J. M. (1994) *J. Biol. Chem.* **269,** 22913–22916
47. Sawin, K. E., LeGuellec, K., Philippe, M., and Mitchison, T. J. (1992) *Nature* **359,** 540–543